P6.16 A 16-YEAR CLIMATOLOGY OF GLOBAL RAINFALL FROM SSM/I HIGHLIGHTING MORNING VERSUS EVENING DIFFERENCES

Andrew J. Negri[1*], Robert F. Adler[1], and J. Marshall Shepherd[1]
George Huffman[2], Michael Manyin[2], and Eric J. Nelkin[2]

[1]Laboratory for Atmospheres, NASA/GSFC, Greenbelt, MD
[2]Science Systems and Applications, Inc., Lanham, MD

1. INTRODUCTION

This paper presents the results of an analysis of 16 years of passive microwave observations from the Special Sensor Microwave Imager (SSM/I), an instrument aboard a succession of Department of Defense (DOD) polar orbiting satellites. Our objectives are threefold:

1. To present the climatology of rainfall estimated by this sensor for the period July 1987 through December 2003, using only the observations at 06 and 18 local time (LT). No observations were available (at these times) during December 1987 and between March 1990 and December 1991.

2. To present the amplitude (AMP) of the diurnal cycle of rainfall, as exemplified by the difference between the 18 (PM) and 06 (AM) LT observations.

3. To examine the differences in total rainfall between periods of high Niño 3.4 Index and periods of low Index. Additionally, two periods, the El Niño during October-December (OND) 1997 and the La Niña during OND 1988 were examined for differences in AMP. These were the strongest ENSO events observed during the period of SSM/I observations.

Rainfall estimates were produced using the Goddard Profiling (GPROF) algorithm version 6 (Kummerow et al, 1996, Olson et al, 1999) and aggregated from the original 12.5 km resolution to 0.5°.

In earlier studies, Negri et al (1994) examined warm season rainfall and its diurnal variation using 3-5 years of SSM/I observations, and Negri et al (2000) looked at 10 years of SSM/I estimates over the Amazon basin.

2. RESULTS

a) The mean rainfall

Figure 1 displays the mean rain rate (mm/month) derived from both the AM and PM overpasses of the SSM/I. Note that the scaling is logarithmic. For presentation and clarity, the globe is broken up into three sections, each of 120° latitude (60N-60S) and 120° longitude.

The main features of the planetary circulation are clearly visible: the ITCZ, SPCZ, enhanced rainfall over continental Africa, South America, and the Maritime Continent. This version of GPROF often mistakenly identifies as rainfall cold land surfaces, such as Hudson Bay in Canada, and also arid regions along coastlines, for example in Africa along the northern coast and Lake Nasser.

b) The amplitude of the diurnal cycle

In Figure 2 we present the difference between the PM and AM observations, suggesting that this be used as a proxy for the amplitude of the diurnal cycle. The units are mm/month, and the scaling is linear.

Interesting diurnal variations are most readily visible over the islands of the Maritime Continent: Indonesia and New Guinea. Liberti et al (2001), Ohsawa et al (2001), and Hadi et al (2002) have previously noted this land/sea effect on the diurnal cycle. Other areas of coastal effects include both coasts of Central America. The effect is enhanced by concavities in the coastline, for example in the Gulf of

*Corresponding author address: Andrew J. Negri; NASA/GSFC Code 912, Greenbelt, MD 20771, email: andrew.negri@nasa.gov

Panama and the Gulf of Guinea (Africa), quite possibly two of the rainiest spots on the planet.

Along the northern coast of Brazil, the effects of coastal squall lines are evident, as is the mountain/valley circulation associated with the Andes Mountains. There is a clear preference for morning rainfall in the equatorial Pacific Ocean.

c) ENSO related differences

Using the Niño 3.4 Index, months were classified as either top third (Niño 3.4 > 0.36) or bottom third (Niño 3.4 < 0.32), and aggregated accordingly. Only the months of October to January were included. The difference between these two extremes is presented in Figure 3, for the 6 AM (top) and 6 PM (bottom) estimates. The main features of this analysis include the decrease in precipitation over the Maritime Continent and increases over the equatorial Pacific and Indian Oceans. There is a decrease in rainfall over Amazonia and a slight increase over the Southeast U.S. The patterns are approximately the same in both the AM and PM composites.

d) Latitudinal profiles of rainfall

We examine the hypothesis that the amplitude of the diurnal cycle will be affected by ENSO variations, due to its unequal effect on land and ocean. To examine this hypothesis, we chose two extremes, the period OND 1997 (El Niño) and OND 1988 (La Niña). Results are presented in Figure 5, the difference in AMP between these two periods. (Note that AMP = PM minus AM estimates). Results at the 0.5° are complicated, and are undergoing further examination and statistical significance analysis. Figures 4 and 5 show the latitudinal profiles of land and oceanic rainfall, respectively. The mean rainfall for each graph is shown in the upper left corner.

We find no statistically significant difference between the two extreme ENSO variations in the global mean (land or ocean) for AM, PM or AMP rainfall. Increases in land rainfall during La Niña are noted near the equator in both the AM and PM estimates, no effect in the Northern Hemisphere and a decrease in the Southern Hemisphere sub-tropics. The only place with large differences in over-land rainfall diurnal cycle is the region between 30° and 40° S, i.e. sub-tropical South America.

Over the ocean (Figure 5), we see both a shift to the south and an increase in rainfall during the El Niño, more prominently in the AM profile. Virtually no differences in AM or PM rainfall are noted in the mid-latitude oceans during ENSO variations.

CONCLUSIONS

The major conclusions of this research are:

- The most striking diurnal variations (18 LT – 06 LT) on the planet were found over the islands of the Maritime Continent: Indonesia and New Guinea.
- Significant (and previously known) differences in rainfall between El Niño and La Niña periods are revealed in the GPROF rain estimates
- We find no statistically significant difference between the two extreme ENSO variations in the global mean (land or ocean) for AM, PM or AMP rainfall.

ACKNOWLEDGEMENTS - The authors acknowledge the continued support of Dr. Ramesh Kakar, NASA/HQ Program Manager for Atmospheric Dynamics and Remote Sensing.

REFERENCES

Hadi, T.W., T. Horinouchi, T. Tsuda, H. Hashiguchi and S. Fukao, 2002: Sea-breeze circulation over Jakarta, Indonesia: A climatology based on boundary later radar observations, *Mon. Wea. Rev,* **130**, 2153-2166.

Kummerow, C., W.S. Olson, and L. Giglio, 1996: A simplified scheme for obtaining precipitation and vertical hydrometeor profiles from passive microwave sensors. *IEEE Trans. Geosci. Remote Sens.*, **34**, 1213-1232.

Liberti, G.L., F. Cheruy and M. Debois, 2001: Land effect on the diurnal cycle of clouds over the TOGA COARE area as observed from GMS IR data, *Mon. Wea. Rev,* **129**, 1500-1517.

Negri, A.J., R.F. Adler, E.J. Nelkin and G.J. Huffman, 1994: Regional rainfall climatologies derived from Special Sensor Microwave Imager (SSM/I) data. *Bull. Amer. Meteor. Soc.,* **75**, 1165-1182.

Negri, A.J., E.N. Anagnostou, and R.F. Adler, 2000: A 10-year Climatology of Amazonian Rainfall Derived from Passive Microwave Satellite Observations. *J. Appl. Meteor.*, **39**, 42-56.

Ohsawa,T., H. Ueda, T. Hayashi, A. Watanabe and J. Matsumoto, 2001: Diurnal variations of convective activity and rainfall in tropical Asia, *J. Met. Soc. Japan*, **79**, 333-352.

Olson, W.S., C.D. Kummerow, Y. Hong, and W.-K. Tao, 1999: Atmospheric latent heating distributions in the tropics derived from satellite passive microwave radiometer measurements. *J. Appl. Meteor.*, **38**,633-664.

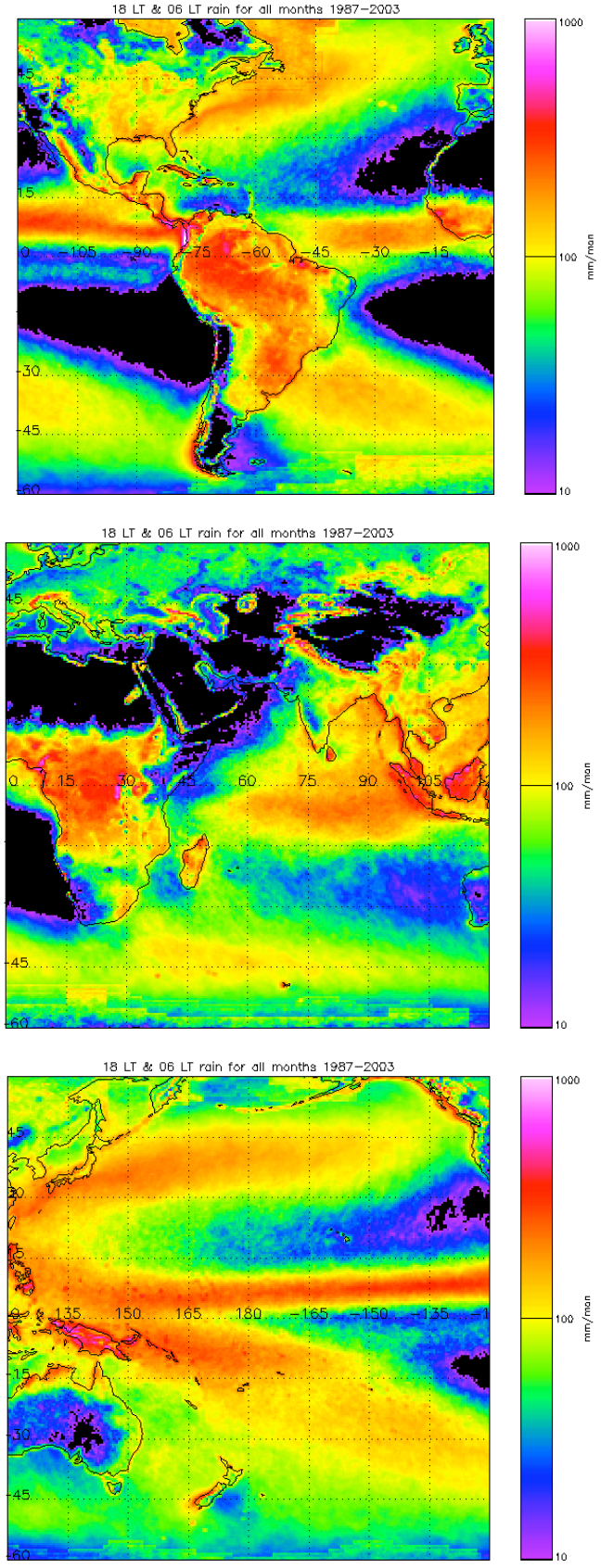

Figure 1. Mean rain rate (mm/month) for 1987-2003 from 06 LT and 18 LT SSM/I overpasses

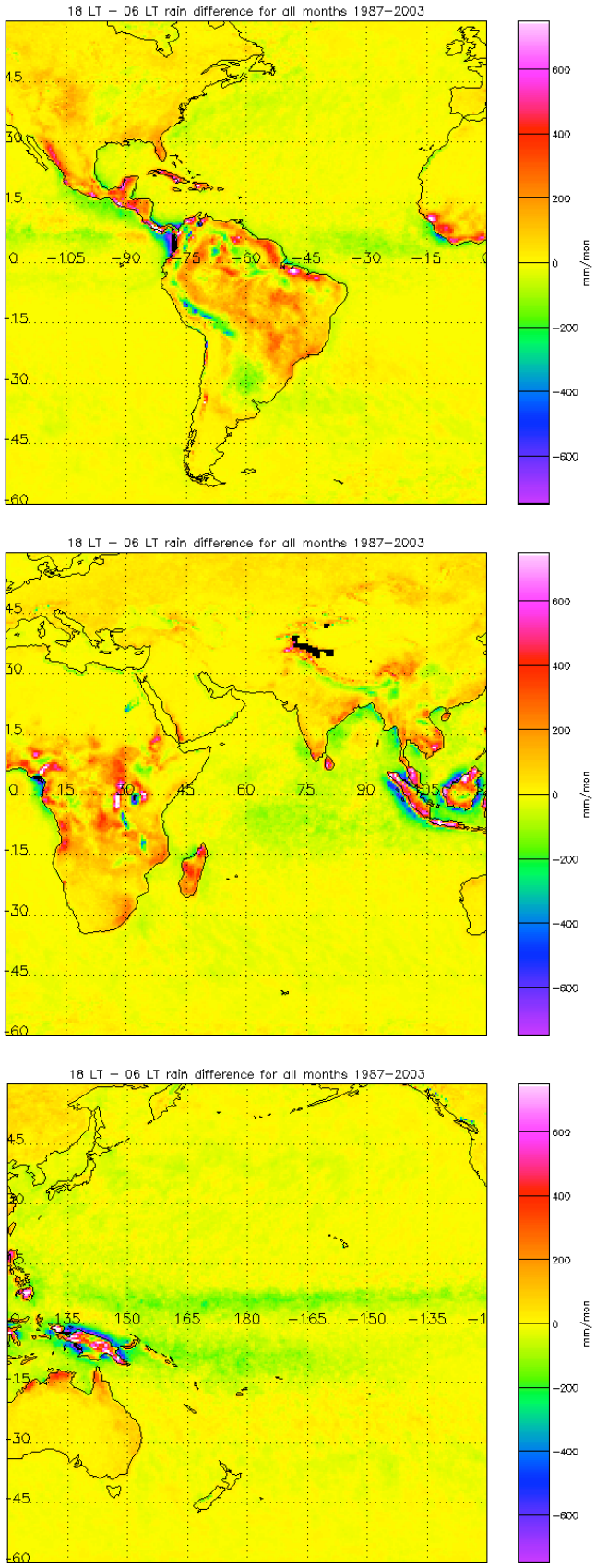

Figure 2. Mean rain difference (18 – 06 LT, in mm/month) 1987 to 2003

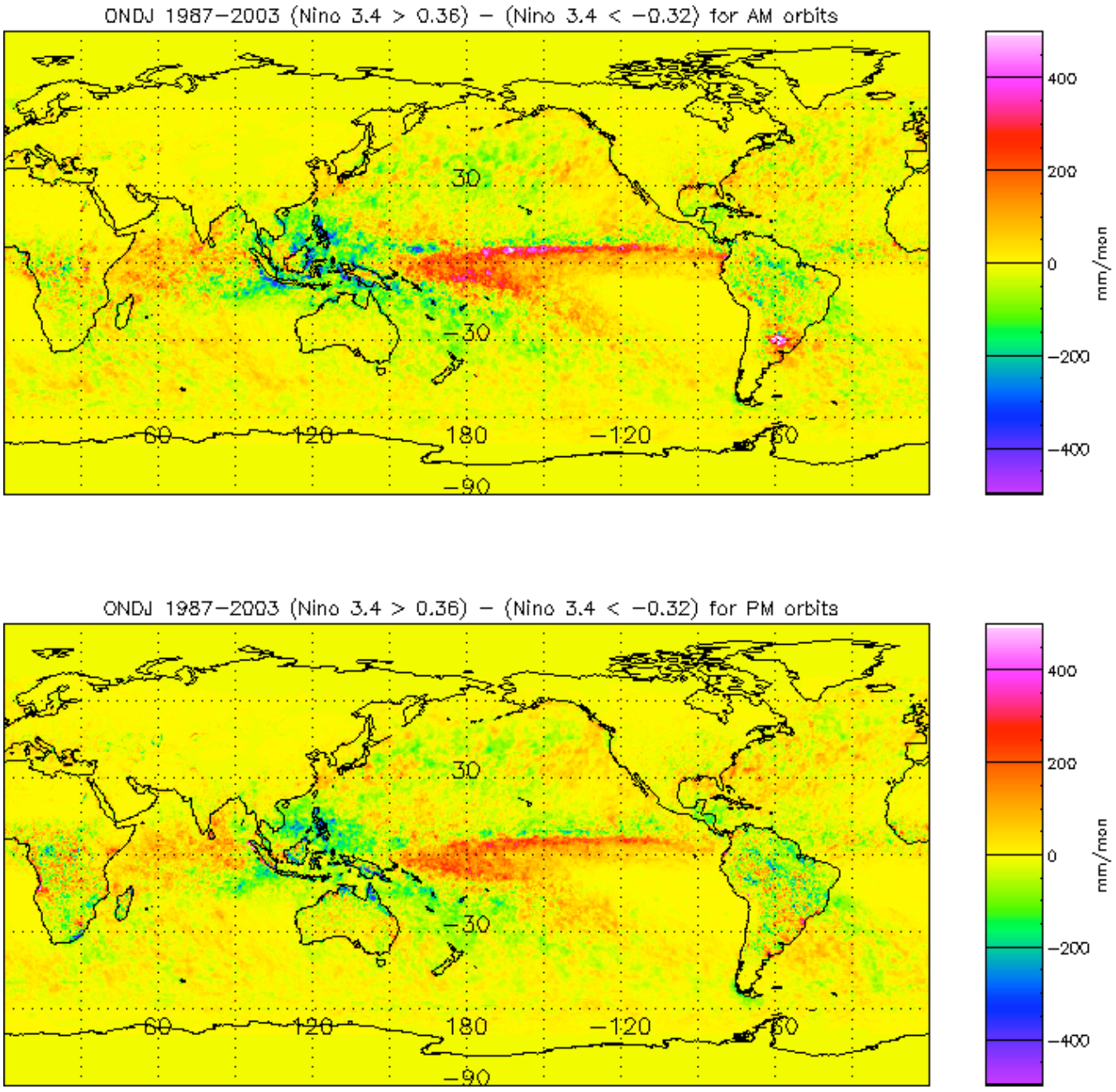

Figure 3. Rain estimates for high Niño *Index minus low* Niño *Index for 06 LT data (top) and 18 LT data (bottom). Only the months of October through January were included in the analysis*

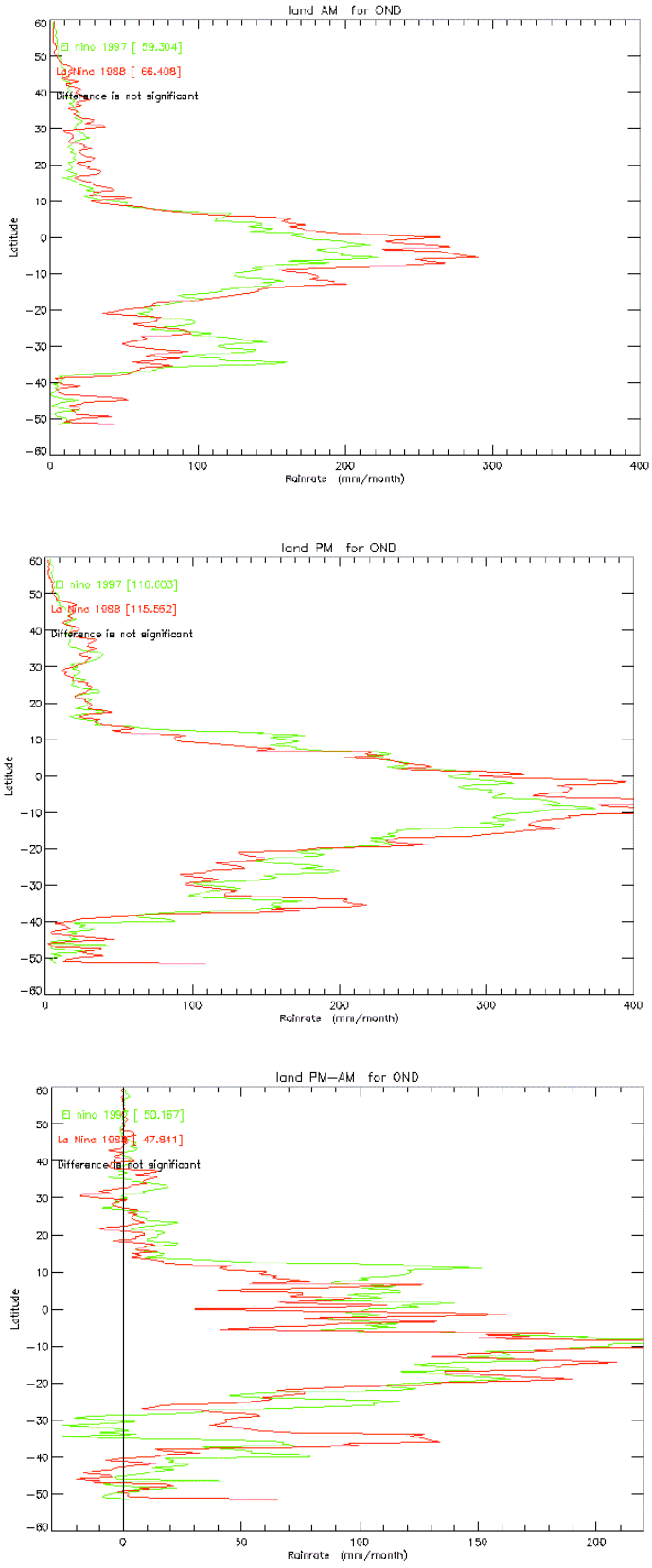

Figure 4. Latitudinal profiles of land-only rainfall for 18 LT (top), 06 LT (middle) and 18 LT – 06 LT (bottom). The 1997 El Niño is plotted in green, the 1988 La Niña event in red.

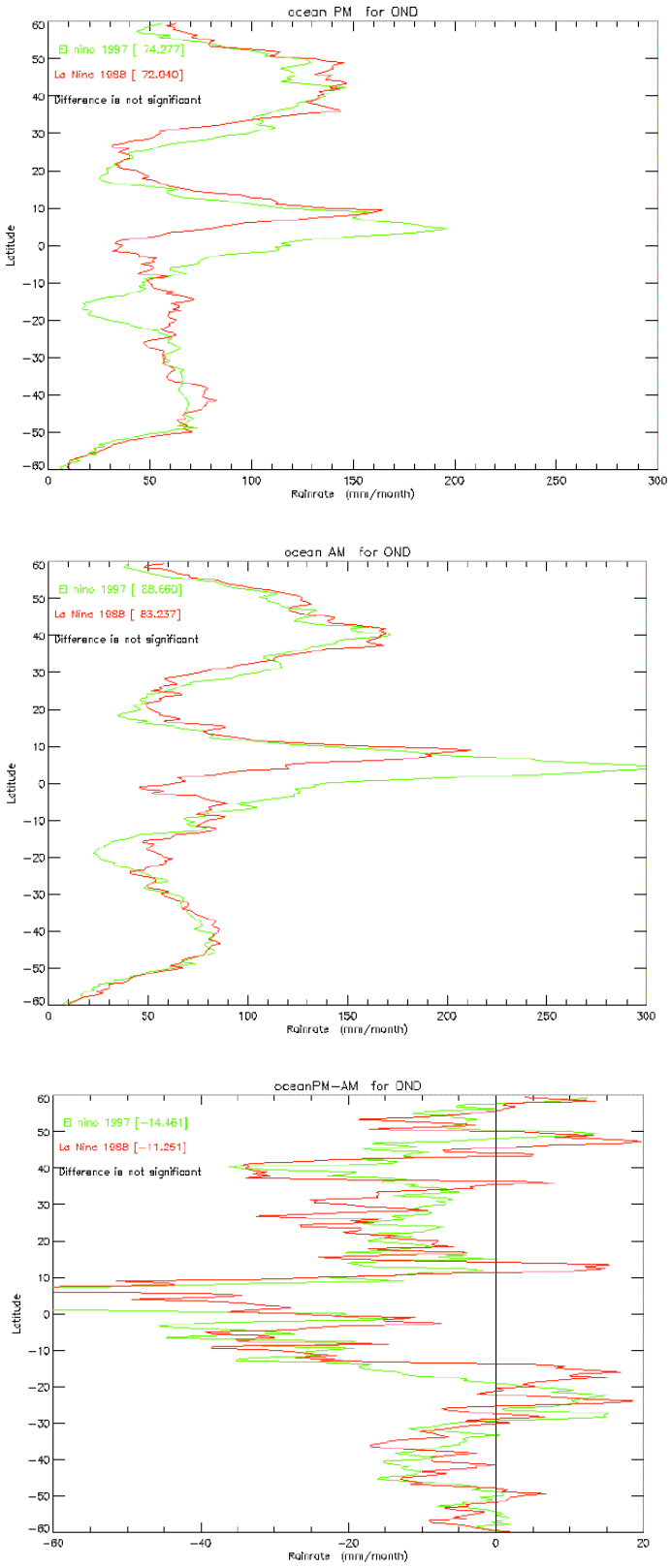

Figure 5. Latitudinal profiles of ocean-only rainfall for 18 LT (top), 06 LT (middle) and 18 LT – 06 LT (bottom). The 1997 El Niño is plotted in green, the 1988 La Niña event in red.